

# Deterministic Active Matter Generated Using Strange Attractors

Rahil N. Valani<sup>1\*</sup> and David M. Paganin<sup>2</sup>

<sup>1</sup>*School of Mathematical Sciences, University of Adelaide, South Australia 5005, Australia and*

<sup>2</sup>*School of Physics and Astronomy, Monash University, Victoria 3800, Australia*

(Dated: November 25, 2024)

Strange attractors are induced by governing differential or integro-differential equations associated with non-linear dynamical systems, but they can also drive such dynamics. When the governing equations contain stochastic forcing, they may also be replaced by deterministic chaotic driving via a governing strange attractor. We outline a flexible deterministic means for such chaotic strange-attractor driven dynamics, and illustrate its utility for modeling active matter. Several active-matter phenomena may be modeled in this manner, such as run-and-tumble particles, run-reverse-flick motion, clustering, jamming and flocking.

Stochastic processes involve systems that undergo probabilistic fluctuations as they evolve in time. This is a widely used framework to model phenomena that vary or appear to vary in a random manner, with applications in biology [1, 2], physics and chemistry [3], ecology [4], neuroscience [5] and finance [6]. Another application is to the emerging field of active matter [7–9]. Active matter refers to a large collection of active particles where each individual particle is a self-propelled entity that consumes energy from its surroundings and converts it into directed motion. Examples of active particles include motile living organisms such as humans, birds, fish or microorganisms such as sperm cells, bacteria and algae, as well as artificial autonomous entities such as active colloidal particles [10], microrobots [11] and walking droplets [12, 13]. Active matter exhibits emergent collective phenomena such as bird flocks, mammalian herds, fish schools, insect swarms, bacterial colonies, swarming robots [14–16], motility-induced phase separation (MIPS) in active colloids [17] and self-organization of microtubules and motors [18, 19].

Self-propulsion of an individual active particle is typically modeled using a stochastic description. For example, a common minimal active-particle model is run-and-tumble particle (RTP) motion, also known as persistent diffusion [20] or dichotomous diffusion [21]. Here, in one dimension, the overdamped stochastic dynamics of the active particle is governed by the Langevin equation [22]

$$\dot{x}(t) = u \sigma_s(t),$$

where an overdot denotes differentiation with respect to time  $t$ ,  $x$  is the position of the active particle,  $u$  is a constant self-propulsion speed and  $\sigma_s(t)$  is a dichotomous Markov noise term that flips between  $-1$  and  $+1$ , following a constant-rate Poisson process. In two dimensions, the RTP “runs” at constant speed in a fixed direction and then instantaneously “tumbles”, i.e. reorients itself by choosing an angle randomly and isotropically [23, 24]. Such RTPs undergo ballistic motion over short times, while diffusive motion emerges at long times [20]. Two

other widely used minimal models of active particles are Active Brownian particles (ABPs) [25] and Active Ornstein-Uhlenbeck particles (AOUPs) [26].

Although a stochastic description is the norm for producing random walks and the corresponding diffusive behavior of active particles, similar features can also emerge from deterministic chaotic processes. Several investigations have documented Brownian-like motion from deterministic dynamics [27–31]. These models include the motion of a particle subjected to a deterministic but chaotic force. Deterministic diffusive motion also arises in Lorenz-like dynamical systems [32] as well as in a system of delay differential equations [33]. Recently, deterministic diffusion was observed in simulations of walking droplet dynamics governed by an integro-differential equation of motion [34–38].

Walking droplets [12, 13], also known as walkers, are a fascinating hydrodynamical active-matter system. In this system, the active particles are self-propelled millimetric droplets walking horizontally on the surface of a vertically vibrating liquid bath. The walker, upon each bounce, generates a localized slowly decaying standing wave. The walker interacts with these self-generated waves on subsequent bounces to propel itself horizontally. At high vibration amplitudes, the waves created on each bounce decay very slowly in time and the walker’s motion is not only influenced by the wave created on its most recent bounce, but also by the waves it created in the distant past, giving rise to memory in the system. In the high-memory regime, walkers mimic several peculiar features that were previously thought to be exclusive to the quantum realm [39]. An idealized theoretical model that captures the key dynamics of a walking droplet is [34, 35, 40]

$$\kappa \ddot{x} + \dot{x} = \frac{\beta}{2} \int_{-\infty}^t \sin(x(t) - x(s)) e^{-(t-s)} ds. \quad (1)$$

This dimensionless equation of motion describes one-dimensional horizontal dynamics of a walker located at  $x$ , which continuously generates waves with cosine-function spatial form that decay exponentially in time. The left side comprises an inertial term  $\kappa \ddot{x}$  and a drag term  $\dot{x}$ . The right side quantifies the forcing on the droplet due

\* rahil.valani@adelaide.edu.au

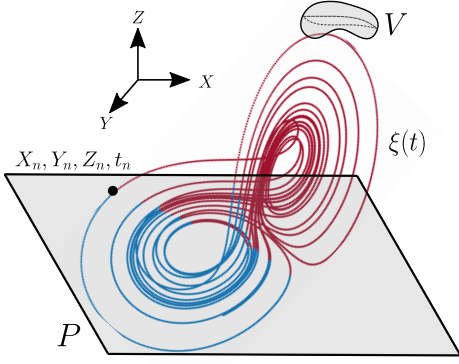


FIG. 1. Asymptotic evolution of the state-space trajectory  $\xi(t) = (X(t), Y(t), Z(t))$  towards the strange-attractor set induces trigger times  $t_n$  such that  $\xi(t_n) \in P$  or  $\xi(t_n) \in V$ , where  $P$  is a specified plane and  $V$  is a specified volume. The induced trigger times  $t_n$ , together with  $N$  arbitrary functions  $f_j(t_n, \xi(t_n), \xi(t_n), \xi(t_n), \dots)$ ,  $j = 1, \dots, N$  of the strange-attractor trajectory at the trigger times, drive the spatio-temporal evolution of our deterministic active-matter model.

to the underlying wave field, which is proportional to the gradient of the underlying field. Since this model takes into account the waves generated from all previous impacts, the underlying wave field is calculated through integration of waves generated from all the previous bounces of the walker. The two parameters,  $\kappa$  and  $\beta$ , may be interpreted as the ratio of inertia to drag and the ratio of wave forcing to drag respectively.

Valani *et al.* [34] showed that the walker's integro-differential equation of motion in Eq. (1) can be transformed to the following system of ODEs (see Supplemental Material Sec. I [41] for a derivation):

$$\begin{aligned} \dot{x} &= X, \quad \dot{X} = \sigma(Y - X), \\ \dot{Y} &= -XZ + rX - Y, \quad \dot{Z} = XY - bZ. \end{aligned} \quad (2)$$

These ODEs are the classical Lorenz equations [42] coupled with the droplet position. The  $X$  variable in the Lorenz system is equivalent to the droplet's velocity  $\dot{x}$  while the  $Y$  and  $Z$  variables are related to the memory forcing. The parameters  $\sigma, r, b$  in the Lorenz system are related to the walker's system via  $\sigma = 1/\kappa$ ,  $r = \beta/2$  and  $b = 1$ . Thus the walker's motion can be interpreted to be driven by the velocity  $X$  which is evolving on the Lorenz strange attractor and gives rise to its deterministic diffusive behavior.

Inspired by the emergence of deterministic diffusion with an induced Lorenz strange attractor in the walking-droplet system, this Letter presents a new class of active particles and the resulting active matter, where the conventional stochastic driving is replaced with deterministic chaotic driving by an underlying strange attractor.

We start by proposing a general method to drive an active particle using a governing strange attractor. As shown in Fig. 1, consider a general strange attractor of a chaotic dynamical system. A typical trajectory  $\xi(t)$

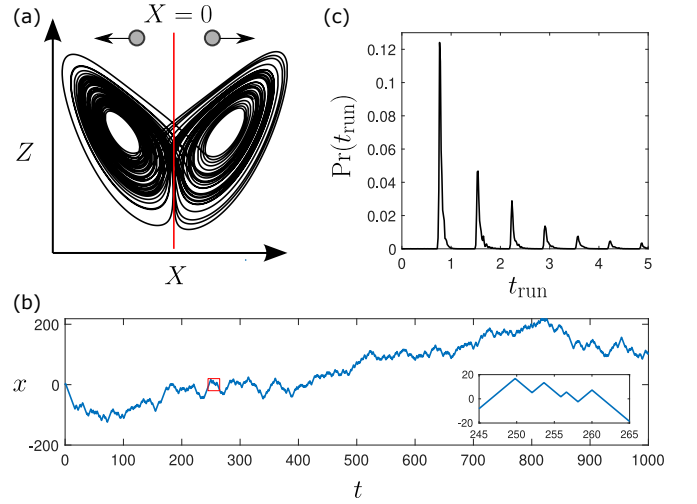


FIG. 2. One-dimensional deterministic RTP-like motion of an active particle driven by the Lorenz strange attractor. (a) The Lorenz attractor with parameters  $\sigma = 10, b = 8/3, r = 28$  drives an active particle moving in one-dimension with a constant speed  $u = \sqrt{r-1}$ , that reverses walking direction when the state-space attractor trajectory crosses the  $X = 0$  plane. (b) Typical space-time trajectory. (c) Probability distribution of time spent in constant-speed ballistic motion between direction reversals.

evolves on this strange attractor. We consider an arbitrary plane  $P$  that cuts through this strange attractor or an arbitrary volume element  $V$  that has a non-zero measure of the strange attractor enclosed within it. Let  $t_n$  be the times when the trajectory on the strange attractor intersects the plane  $P$  or enters the volume element  $V$  for the  $n$ th time. We use these times  $t_n$  as trigger events for the active particle. Such triggers could be to change the direction of motion of the active particle and/or employ a measurable of the chaotic attractor at the trigger event to select the corresponding variable of the active particle after the trigger event. For example, the new direction of motion at time  $t_n$  may be a function of (i) the angle between  $P$  and the tangent to  $\xi(t)$  at  $t = t_n$ , or (ii) the curvature of  $\xi(t_n)$  at  $P$ , or (iii) the time spent within the state-space volume  $V$ , etc. In this way, one can construct a broad class of generic active-particle motion, driven by a strange attractor in an entirely deterministic manner.

We now apply this formalism to a one-dimensional active particle. The RTP in one-dimension has been studied extensively [43–48]. We here generate RTP-like motion in one dimension using the Lorenz strange attractor. We coarse-grain the system in Eq. (2) by only considering the sign of  $X$  for the first equation, giving

$$\dot{x} = u \sigma_d(t), \quad (3)$$

where  $\sigma_d(t) = \text{sgn}(X)$  and  $u$  is a constant denoting the self-propulsion speed of the active particle. This gives rise to one-dimensional RTP-like dynamics where the particle moves to the left or the right with a constant speed  $u$  and switches direction when the sign of the variable  $X$

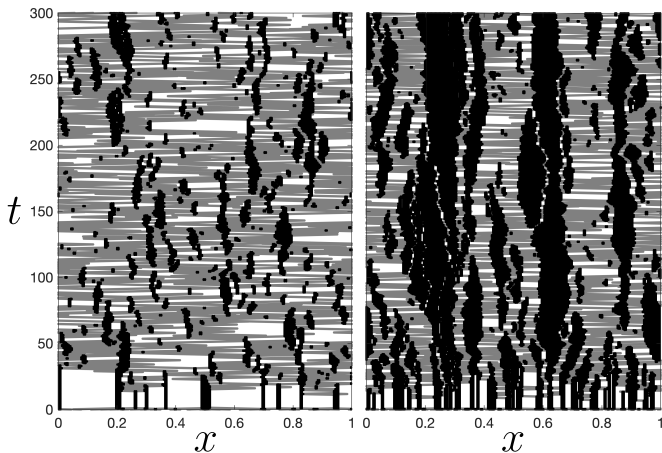


FIG. 3. Interactions of many 1D active particles on the unit interval with periodic boundary conditions. Adding excluded-volume interactions (see Supplemental Material Sec. II [41]) in the Lorenz-attractor-driven active particles described in Fig. 2 with  $u = 0.2$ , clustering and jamming emerges. Space-time trajectories show the development of small-scale short-lived clusters for 50 particles (left), while long-lived large clusters emerge for 100 particles (right). The gray trajectories denote isolated particles while the black trajectories denote clusters. The size of each particle is 0.005.

from the Lorenz system flips, i.e. when a trajectory on the Lorenz strange attractor switches basin of attraction (see Fig. 2(a)).

Figures 2(b)-(c) show a typical space-time trajectory and the corresponding probability distribution of run lengths for this Lorenz-attractor-driven particle. For a conventional RTP driven by a Markov dichotomous process, the run lengths between direction changes are exponentially distributed. However, for the RTP generated via our Lorenz-attractor-driven model, the distribution of run lengths is inherent to the attractor and here results in a distribution with spikes at discrete time intervals, having an exponential decay envelope (see Fig. 2(c)). These spikes emerge because once the particle switches from one basin of the attractor to another, it performs a discrete number of orbits in that basin, before switching basins again. This simple formalism employed with different strange attractors can generate a wide variety of active particles in one-dimension such as ABP-like motion and AOUP-like motion (see Supplemental Material Sec. III [41]). Note that the attractors, arising from these induced motions, will in general differ from the driving attractor. Similarly, the emergent equations induced by our model will differ from those used to construct the driving attractor.

Emergent behavior is a feature of active-matter systems, that arises when interactions are encoded at the level of individual active particles. For example, in one-dimension, interaction of many RTPs with purely repulsive excluded-volume interactions results in clustering and jamming [49–51], while introducing simple align-

ing rules gives rise to one-dimensional flocking states that can stochastically change direction [52]. Moreover, purely repulsive interactions of various active particles in one-dimension can give rise to motile and dynamic clusters [53]. We can readily include purely repulsive interactions in our 1D strange-attractor-driven RTPs. For example, Fig. 3 shows spatiotemporal plots of many interacting 1D Lorenz-attractor-driven active particles described in Fig. 2, via an added excluded-volume interaction [41]. We see the emergence of clustering and jamming. For smaller numbers of particles we observe short-lived small clusters. Increasing the particle density leads to longer-lived larger clusters. By including short-range spring-like interactions we also obtain dynamic and motile clusters, while introducing aligning interactions results in flocking states (see Supplemental Material Sec. III [41]).

We now extend this formalism to two spatial dimensions. As an indicative example, in 2D the  $x$  and  $y$  coordinates of the particle may be taken to evolve via

$$\dot{\mathbf{x}} = (\dot{x}, \dot{y}) = (u \cos(\theta(t)), u \sin(\theta(t))).$$

Here,  $u$  is a constant speed and the angle  $\theta(t)$  is now a dynamical variable linked to a strange attractor. We construct 2D active particles by choosing turning angles  $\Delta\theta_n$  at times  $t_n$  when a trajectory on the Lorenz strange attractor crosses the plane  $X = 0$ . We can choose the turning angle in various ways, e.g.  $\Delta\theta_n = Z(t_n) \bmod(2\pi)$  results in a trajectory shown in Fig. 4(a). This 2D RTP-like active particle undergoes ballistic motion at short times and diffusive motion at longer times. Instead of determining the turning angle directly from the strange attractor, one can also construct a trajectory based on a prescribed probability distribution of turning angles. For example, we can generate run-reverse-and-flick motion by alternating between two different turning angles. We choose the turning angle to be  $\pm\Delta\theta_1$  at trigger times  $t_{2k}$  and  $\pm\Delta\theta_2$  at trigger times  $t_{2k+1}$ , where  $k$  is any natural number. We simulate two different trajectories on the Lorenz strange attractor at the same parameter values but different initial conditions. This results in the evolving trajectories  $\xi_0(t) = (X_0(t), Y_0(t), Z_0(t))$  and  $\xi_1(t) = (X_1(t), Y_1(t), Z_1(t))$ . When the trajectory  $\xi_0(t)$  hits the plane  $X_0 = 0$ , it acts as a trigger to cease the run phase and choose a turning angle according to  $\Delta\theta = 0.5(\Delta\theta_2 - \Delta\theta_1) \text{sgn}(X_1) \text{sgn}(X_0) + 0.5 \text{sgn}(X_1)(\Delta\theta_2 + \Delta\theta_1)$ . By choosing  $\Delta\theta_1 = 71^\circ$  and  $\Delta\theta_2 = 178^\circ$  we obtain a trajectory similar to run-reverse-flick motion of bacteria [55], as shown in Fig. 4(b). We can also use the trigger times  $t_n$  to generate arbitrary turning-angle distributions (see Supplemental Material Sec. IV [41]). Using different strange attractors we can generate active-particle trajectories of different types. For example Fig. 4(c) shows a Lévy walk-like intermittent trajectory generated using the Bouali attractor [54] with a uniform turning angle distribution. Here the particle alternates between phases of a long “run” where it undergoes ballistic motion and “explore” phase where the particle explores a localized region of

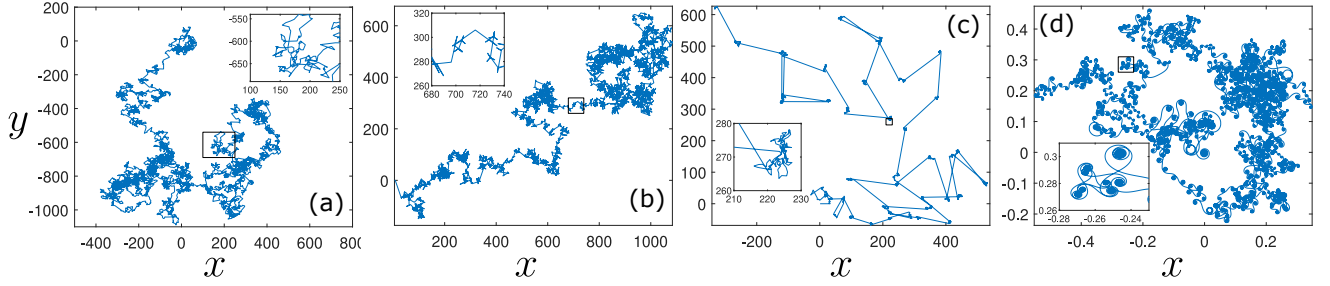


FIG. 4. Two-dimensional deterministic active particles. (a) Active particle trajectory generated from the Lorenz system with parameters  $\sigma = 10$ ,  $b = 8/3$  and  $r = 28$ , where both run lengths and turning angles are determined from the underlying Lorenz attractor. (b) Active particle driven in the same way as in (a) except that the turning angles are prescribed to alternate between  $\pm\Delta\theta_1 = 71^\circ$  and  $\pm\Delta\theta_2 = 178^\circ$  to mimic run-reverse-flick motion. (c) Active particle generated from the Bouali attractor [54] ( $\dot{X} = 3X(1-Y) - 2.2Z$ ,  $\dot{Y} = -(1-X^2)Y$ ,  $\dot{Z} = 0.001X$  with  $X = 1$  as the cutting plane) along with a deterministically generated uniform turning-angle distribution. (d) Active particle generated from the same Lorenz system as (a) but the turning angles are updated continuously, resulting in a curlicued trajectory with long time diffusion.

space. Another example employs a scaled Lorenz system with a Gaussian turning-angle distribution, to generate a 2D ABP-like particle (see Supplemental Material Sec. V [41]). Instead of choosing the turning angle only at trigger times, one can choose the turning angle continuously from the strange attractor, e.g. using  $\Delta\theta(t) = Z(t) \bmod(2\pi)$  which results in a novel type of curlicued random walk with circular and spiral structures as shown in Fig. 4(d).

We can also incorporate interactions in 2D active particles driven by strange attractors. By incorporating aligning interactions we can obtain 2D flocking behavior, as shown in Fig. 5 and Supplemental Video S1. Here, each active particle is driven by the rule described in Fig. 4(a) with added Viscek-like aligning interactions (see Supplemental Material Sec. II [41]). This gives rise to spontaneous flocks that are out of equilibrium. Starting with 1000 active particles randomly positioned in a 2D periodic domain with random alignments, we initially obtain coherent motion as shown in Fig 5(a). Further evolution leads to formation of a few dense flocks which interact in various ways. As shown in Fig. 5(b), one flock can scatter by interacting with another flock, which results in a net change in direction of the flock. Two flocks can also merge to form a bigger flock. We also observe flock disintegration, where part of the flock leaves and moves in a new direction (see Fig. 5(c)). Moreover, flocks can spontaneously change direction, as shown in Fig. 5(d). By incorporating only repulsive harmonic interactions, we can obtain conventional MIPS as well as more exotic MIPS (see Supplemental Material Sec. V [41] and Supplemental Videos S2 and S3) while repulsive harmonic interactions along with Viscek-like aligning interaction give rise to motile crystals which show various features such as defect dynamics, void formations and soliton-like propagation of alignment disturbances within a cluster (see Supplemental Material Sec. V [41] and Supplemental Video S4).

In this Letter, we presented a simple formalism for gen-

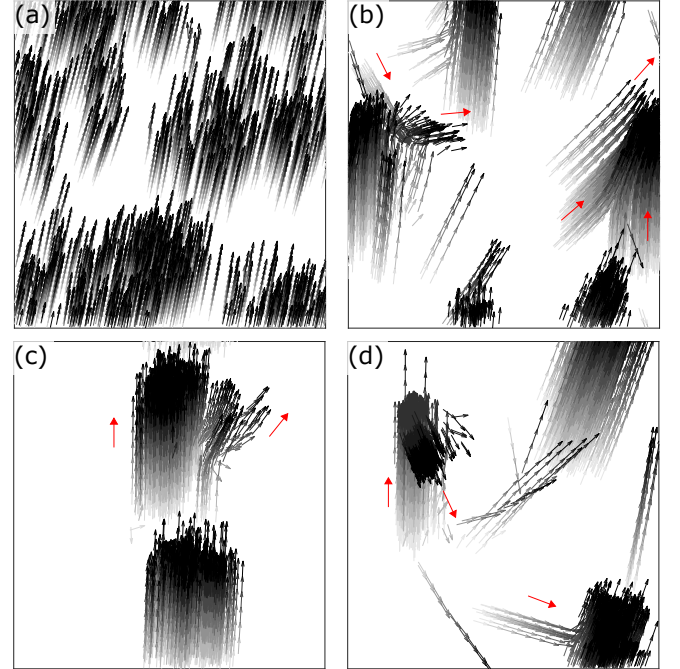


FIG. 5. Two-dimensional flocking of deterministic active particles. 1000 active particles with random initial positions and directions are simulated with aligning interactions of interaction radius  $\Delta = 0.05$  and weight factor  $W = 0.9$  (see Supplemental Material Sec. II [41]) that give rise to (a) coherent flocking initially which is then followed by the formation of dense flocks which can (b) scatter or merge, (c) disintegrate or (d) change flocking direction. The gradient in the grayscale shows the past positions of the active particles with the current position indicated in black. Panels (a)-(d) correspond to  $t = 15.6, 33.4, 36.7$  and  $47.8$ , respectively, in the simulation shown in Supplemental Video S1.

erating active particles driven by strange attractors, and showed some of many phenomena it can model. Although we mainly explored overdamped particle dynamics, iner-



tia can easily be introduced in our active-matter framework. Moreover, we restricted our exploration to dry active matter, but our formalism can also be extended to wet active matter. For example, in the original context of walking droplets, multiple walkers interact with each other via their underlying wave fields. Introducing such wave-mediated interactions in our active-particle formal-

ism may result in novel emergent behaviors for a large collection of particles. Our formalism might also be applied more broadly, beyond the realm of active matter. It would be interesting to explore the engineering of pseudorandom walks, deterministically driven by strange attractors, applied to particular systems in disciplines such as economics, robotics, computer science, chemistry, biology and physics.

- 
- [1] H. C. Berg, *Random Walks in Biology* (Princeton University Press, 2018).
  - [2] L. J. S. Allen, *An Introduction to Stochastic Processes with Applications to Biology* (Chapman and Hall/CRC, 2010).
  - [3] *Stochastic Processes in Physics and Chemistry* (Elsevier, 2007).
  - [4] R. Lande, S. Engen, and B.-E. Saether, *Stochastic Population Dynamics in Ecology and Conservation* (Oxford University Press, 2003).
  - [5] C. Laing and G. J. Lord, eds., *Stochastic Methods in Neuroscience* (Oxford University Press, 2009).
  - [6] T. Rolski, H. Schmidli, V. Schmidt, and J. Teugels, eds., *Stochastic Processes for Insurance & Finance* (John Wiley & Sons, Inc., 1999).
  - [7] S. Ramaswamy, The mechanics and statistics of active matter, *Annu. Rev. Condens. Matter Phys.* **1**, 323 (2010).
  - [8] M. C. Marchetti, J. F. Joanny, S. Ramaswamy, T. B. Liverpool, J. Prost, M. Rao, and R. A. Simha, Hydrodynamics of soft active matter, *Rev. Mod. Phys.* **85**, 1143 (2013).
  - [9] M. R. Shaebani, A. Wysocki, R. G. Winkler, G. Gompper, and H. Rieger, Computational models for active matter, *Nat. Rev. Phys.* **2**, 181 (2020).
  - [10] J. R. Howse, R. A. L. Jones, A. J. Ryan, T. Gough, R. Vafabakhsh, and R. Golestanian, Self-motile colloidal particles: From directed propulsion to random walk, *Phys. Rev. Lett.* **99**, 048102 (2007).
  - [11] S. Palagi and P. Fischer, Bioinspired microrobots, *Nat. Rev. Mater.* **3**, 113 (2018).
  - [12] Y. Couder, S. Protière, E. Fort, and A. Boudaoud, Dynamical phenomena: Walking and orbiting droplets, *Nature* **437**, 208 (2005).
  - [13] R. N. Valani, A. C. Slim, and T. Simula, Superwalking droplets, *Phys. Rev. Lett.* **123**, 024503 (2019).
  - [14] T. Vicsek and A. Zafeiris, Collective motion, *Phys. Rep.* **517**, 71 (2012).
  - [15] T. Vicsek, A. Czirók, E. Ben-Jacob, I. Cohen, and O. Shochet, Novel type of phase transition in a system of self-driven particles, *Phys. Rev. Lett.* **75**, 1226 (1995).
  - [16] H. Chaté, Dry aligning dilute active matter, *Annu. Rev. Condens. Matter Phys.* **11**, 189 (2020).
  - [17] M. E. Cates and J. Tailleur, Motility-induced phase separation, *Annu. Rev. Condens. Matter Phys.* **6**, 219 (2015).
  - [18] T. Surrey, F. Nédélec, S. Leibler, and E. Karsenti, Physical properties determining self-organization of motors and microtubules, *Science* **292**, 1167 (2001).
  - [19] F. J. Ndlec, T. Surrey, A. C. Maggs, and S. Leibler, Self-organization of microtubules and motors, *Nature* **389**, 305 (1997).
  - [20] V. Balakrishnan and S. Chaturvedi, Persistent diffusion on a line, *Physica A* **148**, 581 (1988).
  - [21] I. Bena, Dichotomous Markov noise: Exact results for out-of-equilibrium systems, *Int. J. Mod. Phys. B* **20**, 2825 (2006).
  - [22] A. Dhar, A. Kundu, S. N. Majumdar, S. Sabhapandit, and G. Schehr, Run-and-tumble particle in one-dimensional confining potentials: Steady-state, relaxation, and first-passage properties, *Phys. Rev. E* **99**, 032132 (2019).
  - [23] A. K. Hartmann, S. N. Majumdar, H. Schawe, and G. Schehr, The convex hull of the run-and-tumble particle in a plane, *J. Stat. Mech. Theory Exp.* **2020**, 053401 (2020).
  - [24] I. Santra, U. Basu, and S. Sabhapandit, Run-and-tumble particles in two dimensions: Marginal position distributions, *Phys. Rev. E* **101**, 062120 (2020).
  - [25] P. Romanczuk, M. Bär, W. Ebeling, B. Lindner, and L. Schimansky-Geier, Active Brownian particles, *Eur. Phys. J. Spec. Top.* **202**, 1 (2012).
  - [26] L. L. Bonilla, Active Ornstein-Uhlenbeck particles, *Phys. Rev. E* **100**, 022601 (2019).
  - [27] G. Trefán, P. Grigolini, and B. J. West, Deterministic Brownian motion, *Phys. Rev. A* **45**, 1249 (1992).
  - [28] P. Gaspard, M. E. Briggs, M. K. Francis, J. V. Sengers, R. W. Gammon, J. R. Dorfman, and R. V. Calabrese, Experimental evidence for microscopic chaos, *Nature* **394**, 865 (1998).
  - [29] C. Beck, Dynamical systems of Langevin type, *Physica A* **233**, 419 (1996).
  - [30] L. Chew and C. Ting, Microscopic chaos and Gaussian diffusion processes, *Physica A* **307**, 275 (2002).
  - [31] M. C. Mackey and M. Tyran-Kamińska, Deterministic Brownian motion: The effects of perturbing a dynamical system by a chaotic semi-dynamical system, *Phys. Rep.* **422**, 167 (2006).
  - [32] R. Festa, A. Mazzino, and D. Vincenzi, Lorenz deterministic diffusion, *Europhys. Lett. (EPL)* **60**, 820 (2002).
  - [33] J. Lei and M. C. Mackey, Deterministic Brownian motion generated from differential delay equations, *Phys. Rev. E* **84**, 041105 (2011).
  - [34] R. N. Valani, A. C. Slim, D. M. Paganin, T. P. Simula, and T. Vo, Unsteady dynamics of a classical particle-wave entity, *Phys. Rev. E* **104**, 015106 (2021).
  - [35] M. Durey, Bifurcations and chaos in a Lorenz-like pilot-wave system, *Chaos* **30**, 103115 (2020).
  - [36] M. Durey, S. E. Turton, and J. W. M. Bush, Speed oscillations in classical pilot-wave dynamics, *Proc. Math. Phys. Eng. Sci.* **476**, 20190884 (2020).
  - [37] M. Durey and J. W. M. Bush, Classical pilot-wave dynamics: The free particle, *Chaos* **31**, 033136 (2021).
  - [38] M. Hubert, S. Perrard, M. Labousse, N. Vandewalle,

- and Y. Couder, Tunable bimodal explorations of space from memory-driven deterministic dynamics, *Phys. Rev. E* **100**, 032201 (2019).
- [39] J. W. M. Bush and A. U. Oza, Hydrodynamic quantum analogs, *Rep. Prog. Phys.* **84**, 017001 (2020).
- [40] A. U. Oza, R. R. Rosales, and J. W. M. Bush, A trajectory equation for walking droplets: hydrodynamic pilot-wave theory, *J. Fluid Mech.* **737**, 552 (2013).
- [41] See Supplemental Material at [URL will be inserted by publisher] for videos, technical details of the simulations and additional results.
- [42] E. N. Lorenz, Deterministic Nonperiodic Flow, *J. Atmos. Sci.* **20**, 130 (1963).
- [43] L. Angelani and R. Garra, Run-and-tumble motion in one dimension with space-dependent speed, *Phys. Rev. E* **100**, 052147 (2019).
- [44] K. Malakar, V. Jemseena, A. Kundu, K. V. Kumar, S. Sabhapandit, S. N. Majumdar, S. Redner, and A. Dhar, Steady state, relaxation and first-passage properties of a run-and-tumble particle in one-dimension, *J. Stat. Mech. Theory Exp.* **2018**, 043215 (2018).
- [45] P. Singh and A. Kundu, Generalised ‘arcsine’ laws for run-and-tumble particle in one dimension, *J. Stat. Mech. Theory Exp.* **2019**, 083205 (2019).
- [46] P. Singh, S. Sabhapandit, and A. Kundu, Run-and-tumble particle in inhomogeneous media in one dimension, *J. Stat. Mech. Theory Exp.* **2020**, 083207 (2020).
- [47] L. Angelani, R. Di Leonardo, and M. Paoluzzi, First-passage time of run-and-tumble particles, *Eur. Phys. J. E* **37**, 59 (2014).
- [48] L. Angelani, Confined run-and-tumble swimmers in one dimension, *J. Phys. A Math. Theor.* **50**, 325601 (2017).
- [49] N. Sepúlveda and R. Soto, Coarsening and clustering in run-and-tumble dynamics with short-range exclusion, *Phys. Rev. E* **94**, 022603 (2016).
- [50] R. Dandekar, S. Chakraborti, and R. Rajesh, Hard core run and tumble particles on a one-dimensional lattice, *Phys. Rev. E* **102**, 062111 (2020).
- [51] R. Soto and R. Golestanian, Run-and-tumble dynamics in a crowded environment: Persistent exclusion process for swimmers, *Phys. Rev. E* **89**, 012706 (2014).
- [52] O. J. O’Loan and M. R. Evans, Alternating steady state in one-dimensional flocking, *J. Phys. A Math. Gen.* **32**, L99 (1999).
- [53] P. Dolai, A. Das, A. Kundu, C. Dasgupta, A. Dhar, and K. V. Kumar, Universal scaling in active single-file dynamics, *Soft Matter* **16**, 7077 (2020).
- [54] S. Bouali, A 3D strange attractor with a distinctive silhouette. The butterfly effect revisited (2014), arXiv:1311.6128.
- [55] J. Taktikos, H. Stark, and V. Zaburdaev, How the motility pattern of bacteria affects their dispersal and chemotaxis, *PLoS ONE* **8**, e81936 (2013).

# Supplemental Material for “Deterministic Active Matter Generated Using Strange Attractors”

Rahil N. Valani<sup>1\*</sup> and David M. Paganin<sup>2</sup>

<sup>1</sup>*School of Mathematical Sciences, University of Adelaide, South Australia 5005, Australia and*

<sup>2</sup>*School of Physics and Astronomy, Monash University, Victoria 3800, Australia*

## I. TRANSFORMING THE WALKER’S INTEGRO-DIFFERENTIAL EQUATION INTO A LORENZ-LIKE SYSTEM OF ODES

Here we provide a derivation to transform the walker’s integro-differential equation of motion into a system of ODEs that take the form of the Lorenz system. Consider the walker’s integro-differential equation of motion,

$$\kappa \ddot{x} + \dot{x} = \frac{\beta}{2} \int_{-\infty}^t \sin(x(t) - x(s)) e^{-(t-s)} ds.$$

Denote the wave-memory force by

$$Y(t) = \frac{\beta}{2} \int_{-\infty}^t \sin(x(t) - x(s)) e^{-(t-s)} ds.$$

Differentiating  $Y(t)$  with respect to time and using the Leibniz integration rule, we have

$$\begin{aligned} \dot{Y}(t) &= -\frac{\beta}{2} \int_{-\infty}^t \sin(x(t) - x(s)) e^{-(t-s)} ds \\ &\quad + \frac{\beta \dot{x}}{2} \int_{-\infty}^t \cos(x(t) - x(s)) e^{-(t-s)} ds \\ &= -Y(t) + XW(t), \end{aligned}$$

where  $\dot{x}_d = X$  and

$$W(t) = \frac{\beta}{2} \int_{-\infty}^t \cos(x(t) - x(s)) e^{-(t-s)} ds.$$

Differentiating  $W(t)$  with respect to time, we get

$$\begin{aligned} \dot{W}(t) &= \frac{\beta}{2} - \frac{\beta}{2} \int_{-\infty}^t \cos(x(t) - x(s)) e^{-(t-s)} ds \\ &\quad - \frac{\beta \dot{x}}{2} \int_{-\infty}^t \sin(x(t) - x(s)) e^{-(t-s)} ds \\ &= \frac{\beta}{2} - W(t) - XY(t). \end{aligned}$$

By making a change of variables

$$Z(t) = \frac{\beta}{2} - W(t),$$

we obtain the following system of Lorenz-like ODEs for the walker’s dynamics,

$$\begin{aligned} \dot{x}_d &= X \\ \dot{X} &= \frac{1}{\kappa}(Y - X) \\ \dot{Y} &= -Y + \frac{\beta}{2}X - XY \\ \dot{Z} &= -Z + XY. \end{aligned}$$

## II. DETAILS OF NUMERICAL SIMULATIONS

The simulation results presented in this manuscript were performed by solving the corresponding dynamics of the strange attractor using the inbuilt ode45 solver in **MATLAB**. Along with this Supplemental Material, we have attached example **MATLAB** codes that simulate some of the behaviors presented in this manuscript. In this section, we provide more details for the implementation of the interactions between active particles.

### A. Excluded-volume interactions

Excluded-volume interactions, leading to clustering and jamming phenomena for the multiple 1D RTP-like particles in Fig. 3 of the main text, were implemented as follows:

1. On the unit interval, with periodic boundary conditions, we define the distance  $d_{ij}$  between two particles  $i$  and  $j$  as the shortest distance between them:

$$d_{ij} = \min(|x_i - x_j|, 1 - |x_i - x_j|).$$

2. For each particle, we find the particles that are within a distance  $d$ , i.e.  $d_{ij} < d$ . Here, the distance  $d$  corresponds to the size of each particle.
3. If a pair of particles is approaching head on, and the particles are less than a distance  $d$  apart, then motion ceases for that pair. However, their velocities continue to evolve on the strange attractor, so when either of the particles reverses its direction of motion and moves away from the other particle, the particles can resume their ballistic motion.

\* rahil.valani@adelaide.edu.au

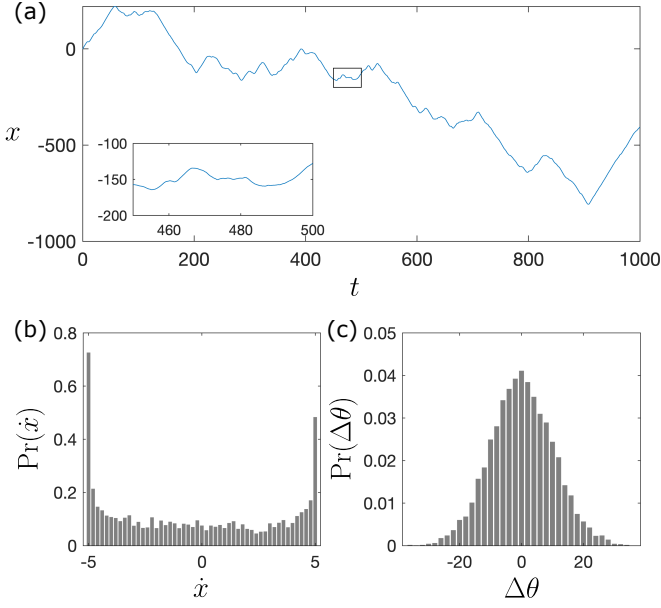


FIG. 1. Deterministic one-dimensional ABP-like particle generated from a scaled Lorenz system with parameters  $\sigma = 10$ ,  $r = 28$ ,  $b = 8/3$  and  $F = 10$ . The one-dimensional trajectory of the particle is shown in (a), while (b) and (c) show the distribution of the particle velocity and the change-in-angle  $\Delta\theta$  respectively. Here the constant speed  $u = \sqrt{r-1}$ . The mean of the Gaussian distribution for  $\Delta\theta$  was chosen to be zero, while the standard deviation was chosen to be  $\sigma_\theta = 10^\circ$ .

### B. Aligning interactions for two-dimensional flocks

Aligning interactions, leading to the flocking behavior in Fig. 5 of the main text, were implemented as follows:

1. For particles in the unit square with periodic boundary conditions, we define the shortest distance between the particles  $i$  and  $j$  as

$$d_{ij} = \sqrt{(X_{ij})^2 + (Y_{ij})^2},$$

where

$$\begin{aligned} X_{ij} &= \min(|x_i - x_j|, 1 - |x_i - x_j|), \\ Y_{ij} &= \min(|y_i - y_j|, 1 - |y_i - y_j|). \end{aligned}$$

2. For each particle, we define a neighborhood which is a circle of radius  $\Delta$ . If there is no other particle inside that neighborhood, then the particle can continue to move as an individual active particle, driven by its strange attractor with its orientation  $\theta(t)$ .
3. If there are other particles in the neighborhood of the  $i$ th particle, then we use a weight factor  $W$  to determine the relative importance that the particle gives to the other particles, compared to its motion

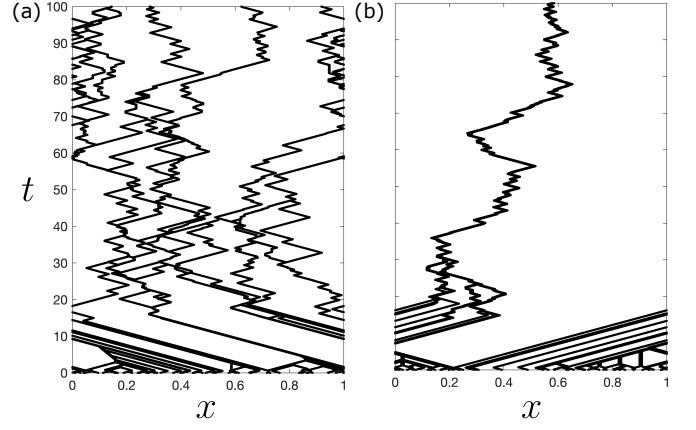


FIG. 2. 1D flocking behavior from aligning interactions of many RTP-like particles driven by the Lorenz strange attractor. (a) Small flocks form which merge and disintegrate for a small flocking-interaction neighborhood of  $\Delta = 0.001$ , while (b) a large single flock is formed for a large flocking-interaction neighborhood of  $\Delta = 0.008$ . The larger single flock in (b) also intermittently changes direction due to the chaotic nature of the attractor. Each particle has a speed of  $u = 0.05$ . The weight factor is  $W = 0.9$ , and the number of particles is 50. The Lorenz attractor parameters are  $\sigma = 10$ ,  $r = 28$  and  $b = 8/3$ .

driven by the strange attractor. The new orientation that the particle chooses is defined as

$$\theta_{\text{new}}(t) = W \theta_{\text{nb}}(t) + (1 - W) \theta(t).$$

Here  $\theta_{\text{nb}}$  is the average direction of the particles in the neighborhood, defined in the same way as the Vicsek flocking model [? ].

## III. ONE-DIMENSIONAL ACTIVE PARTICLES

### A. Active Brownian Particles (ABPs) and Active Ornstein-Uhlenbeck Particles (AOUPs) from strange attractors

Using the formalism for generating one-dimensional RTP-like active particles that is described in the main text, one can also generate an ABP-like particle in a deterministic way using strange attractors. The equation of motion obeyed by a one-dimensional ABP-like particle is [? ]

$$\dot{x} = u \cos(\theta(t)).$$

Here,  $u$  is a constant speed, and  $\theta(t)$  is an internal angular co-ordinate which evolves on a strange attractor and is calculated at each time step using

$$\theta(t_{i+1}) = \theta(t_i) + \Delta\theta(t_i).$$

A trajectory is simulated on a scaled Lorenz strange attractor system given by

$$\begin{aligned}\dot{X} &= F(\sigma(Y - X)) \\ \dot{Y} &= F(-Y + rX - XZ) \\ \dot{Z} &= F(-bZ + XY),\end{aligned}$$

where  $F$  is a non-zero real number. The trigger time  $t_n$  is determined by the intersection of the trajectory along the scaled Lorenz attractor with the cutting plane  $X = 0$ . The change in the internal angular co-ordinate,  $\Delta\theta(t_i)$ , is either (i) zero if the trajectory on the Lorenz strange attractor does not cross the cutting plane  $X = 0$  in the time interval between  $t_{i-1}$  and  $t_i$ , or (ii) we select a value of  $\Delta\theta(t_i)$  from a Gaussian distribution with a mean of 0 and a standard deviation of  $\sigma_\theta$  (using the method described in Sec. IV) if the trajectory intersects the cutting plane during this time interval. This gives an ABP-like motion in one dimension, whose internal angular co-ordinate undergoes rotational diffusion-like behavior with a Gaussian distribution. A typical trajectory for an ABP-like particle generated in this manner, together with its corresponding internal distribution of  $\Delta\theta$ , is shown in Fig. 1.

In a similar way, one can construct a trajectory of an AOUP-like particle using the same scaled Lorenz strange attractor. The equation of motion of a traditional AOUP particle in one-dimension is [?] ]

$$\tau\ddot{x} + \dot{x} = \sqrt{2\Delta}\xi(t).$$

Here  $\xi(t)$  is Gaussian white noise term with zero mean and unit variance,  $\tau$  is a persistent time constant and  $\Delta$  is the strength of the noise term. By using the trigger times  $t_n$  of the scaled Lorenz system, we can generate an approximately Gaussian distribution using the process described in Sec. IV, which in the present context will be the equivalent of the noise term  $\xi(t)$ . Hence, one can create a trajectory for an AOUP-like particle in a deterministic way, driven by strange attractors.

## B. 1D flocks from strange attractors

We can generate one-dimensional flocking behavior [?] ] by including aligning interactions for the one-dimensional RTP-like particles in a periodic domain. We implement the aligning interactions by allowing each such active particle to detect other active particles in a neighborhood of length  $\Delta$  on either side of the particle. If there are no particles in the neighborhood, then the particle continues to evolve according to the RTP-like motion based on the Lorenz strange attractor. Conversely, if there are particles in the neighborhood then we sum the signs of the velocities of each of these particles (right as positive and left as negative) to find the direction of the majority of the particles in the neighborhood. For  $i$ th particle, this quantity is given by  $\sum_{k \neq i} \text{sgn}(X_k)$ . This quantity is then

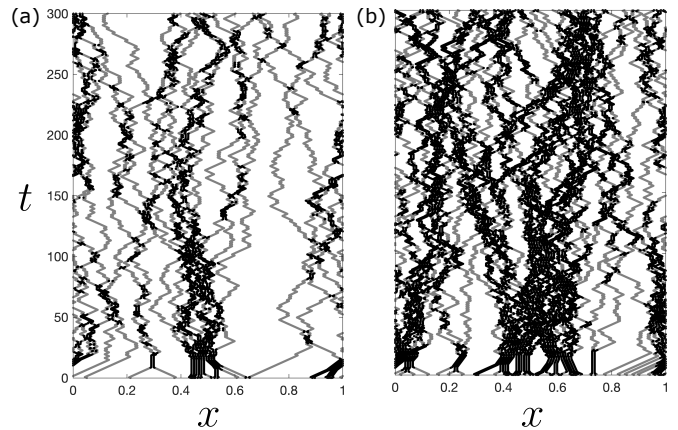


FIG. 3. 1D motile clusters resulting from spring repulsive interactions between RTP-like active particles driven by the Lorenz strange attractor. (a) Small motile clusters form which merge and disintegrate for a small number of particles  $n = 20$ , while (b) larger more persistent clusters form for a larger number of particles  $n = 50$ . Each particle has a speed of  $u = 0.01$ , spring interaction constant  $K = 20$  and interaction distance  $d_c = 0.005$ . The Lorenz attractor parameters are  $\sigma = 10$ ,  $r = 28$  and  $b = 8/3$ . The gray trajectories denote isolated particles while the black trajectories denote clusters.

multiplied by a weight factor  $W$  and added to the product of the particle's own velocity direction  $\text{sgn}(X_i)$  and the corresponding weight factor  $1 - W$ , giving us

$$T_i = W \sum_{k \neq i} \text{sgn}(X_k) + (1 - W) \text{sgn}(X_i).$$

Then  $\text{sgn}(T_i)$  determines the direction of motion of the  $i$ th particle. A typical example of the observed flocking behavior is illustrated in Fig. 2.

## C. 1D motile clusters from strange attractors

In addition to jamming and cluster formation in one-dimension, as described in the main text, we can also generate one-dimensional motile clusters [?] ]. This can be done by including harmonic repulsive interactions between the one-dimensional RTP-like particles, instead of the excluded volume interactions used for Fig. 3 of the main text. We model the repulsive harmonic interactions between particles to activate when the distance between the particles falls below a certain threshold  $2d_c$ , in which case the particles experience a repulsive force according to

$$F_{ij} = K \frac{x_i - x_j}{|x_i - x_j|} (2d_c - |x_i - x_j|).$$

We again ensure that  $|x_i - x_j|$  corresponds to the shortest distance between the particles in the periodic domain, and calculate the spring force accordingly. Figure 3 shows a typical output of simulations where these interactions



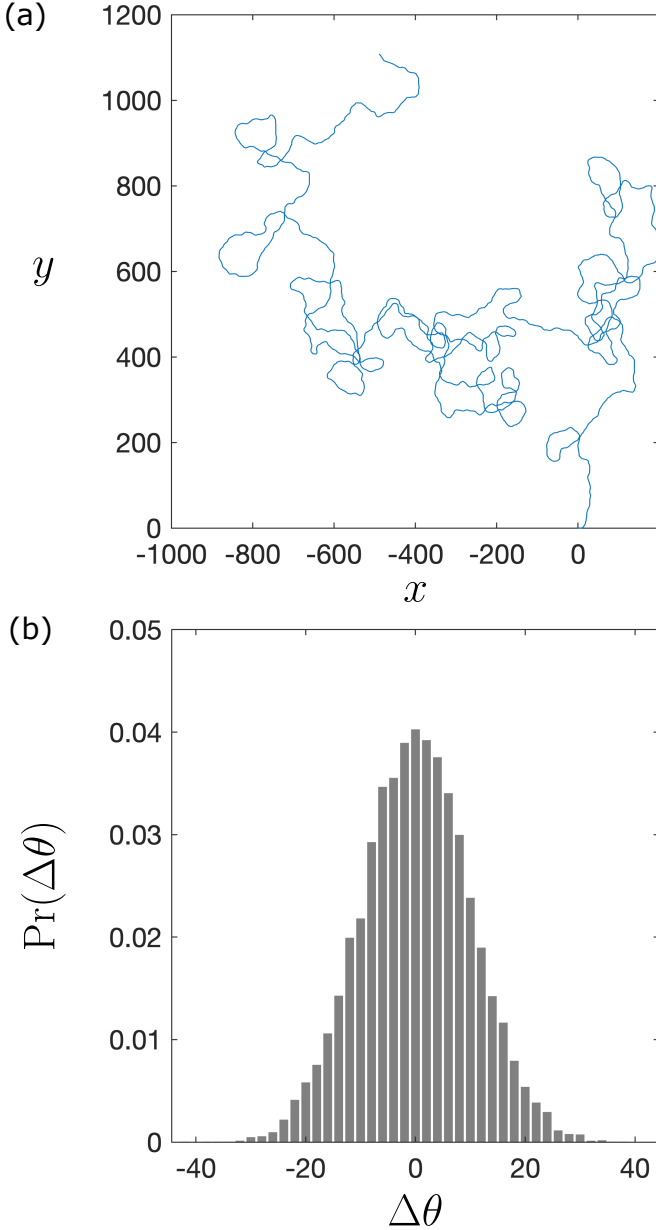


FIG. 4. Two-dimensional ABP-like particle generated from a scaled Lorenz system with parameters  $\sigma = 10$ ,  $r = 28$ ,  $b = 8/3$  and  $F = 10$ . The trajectory of the particle is shown in (a), while (b) shows the probability distribution of the turning angle  $\Delta\theta$ . Here  $u = \sqrt{r-1}$ , the mean of the Gaussian distribution was chosen to be zero, and the standard deviation was chosen to be  $\sigma_\theta = 10^\circ$ .

are modeled between the RTP-like particles. We observe that for a small number of particles, we obtain small-sized transient motile clusters, while for a larger density of particles, we see larger long-lived motile clusters.

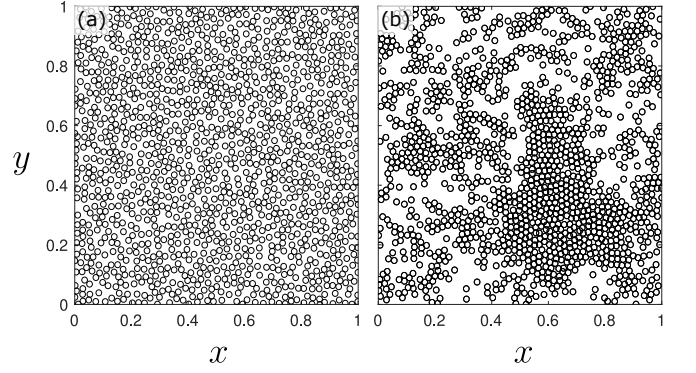


FIG. 5. Two-dimensional interactions of many ABP-like particles resulting in MIPS (see also Supplemental Video S2). (a) Initial state of the system where particles are started randomly, within a unit square with periodic boundary conditions. (b) Emergence of MIPS, where regions of high density and low density are formed due to the repulsive interactions between the ABP-like active particles. The parameters for the ABP-like particles were the same as that described in Fig. 4, and the spring constant for harmonic interactions was taken to be  $K = 50$ .

#### IV. GENERATING ARBITRARY TURNING ANGLE DISTRIBUTIONS DETERMINISTICALLY

We can deterministically generate arbitrary probability distributions for turning angles,  $\text{Pr}(\Delta\theta)$ , using the trigger times  $t_n$  (see Fig. 1 of main text). Let

$$\alpha = \pi(\phi - 1),$$

where

$$\phi = (1 + \sqrt{5})/2$$

is the golden ratio. Now take the trigger times  $t_n$ , divide by a numerical time-step size  $\Delta t$  and round to the nearest integer giving

$$S_n = \text{round}(t_n/\Delta t).$$

We then obtain an approximately uniform-distribution sampling of the turning angles  $\Delta\theta_n$ , using [?] ]

$$\Delta\theta_n = S_n \alpha \bmod(2\pi).$$

We can use this approximately-uniform distribution to generate an arbitrary distribution  $\text{Pr}(\Delta\theta)$ , using the inversion method (see e.g. Chap. 3 of [?]). We start by discretizing the desired distribution, giving

$$P_i = \text{Pr}(\Delta\theta_i).$$

Now, consider laying all these  $P_i$  on a horizontal line in sequence as  $P_1, P_2, \dots$ , where the length of each line segment  $P_i$  is its value. One can now generate an approximately uniform distribution to select a value on this line

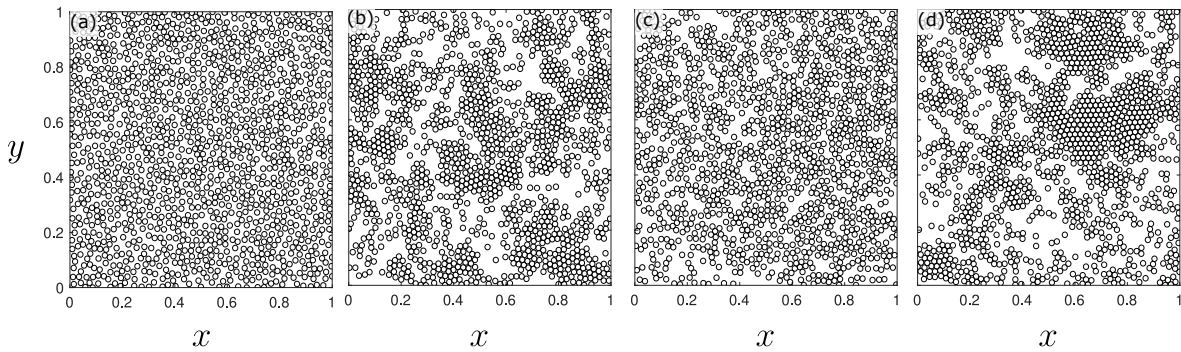


FIG. 6. Emergence of non-equilibrium MIPS behavior when many two-dimensional active particles, driven by the Bouali attractor (see Fig. 4(c) of main text), interact with each other via repulsive harmonic interactions (see also Supplemental Video S3). (a) Initially randomly located active particles interact and result in (b) regions of high and low densities, with MIPS-like behavior when the particles are in the long “run” phase of their motion. (c) These particles then start switching their directions frequently, which results in the disintegration of MIPS-like behavior. (d) After some time, the particles again enter the long “run” phase and resume MIPS. This cycle keeps repeating as the phase space trajectory evolves on the strange attractor. The parameters for the Bouali attractor were the same as in Fig. 4(c) of the main text. The spring constant for the repulsive forces between the particles was chosen as  $K = 50$ .

segment of length  $\sum_i P_i$ , according to

$$R_n = S_n \alpha \bmod \left( \sum_i P_i \right).$$

We identify the line segment  $P_j$  corresponding to length  $R_n$  and sample the corresponding turning angle  $\Delta\theta_j$ . This allows us to deterministically generate pseudorandom numbers from an arbitrary distribution.

## V. TWO-DIMENSIONAL ACTIVE PARTICLES

### A. Two-dimensional ABP

Similar to the one-dimensional ABP-like behavior described in Sec. III A, one can also deterministically generate a two-dimensional ABP-like trajectory for an active particle that is driven by the scaled Lorenz system. We use the same scaled Lorenz system as in Sec. III A and the same Gaussian distribution for the rotational diffusion. Implementing them with the following equation for two-dimensional particle velocity

$$\begin{aligned}\dot{x} &= u \cos(\theta(t)) \\ \dot{y} &= u \sin(\theta(t)),\end{aligned}$$

we get the two-dimensional ABP-like trajectory in Fig. 4.

### B. Motility induced phase separation (MIPS)

Active particles generally accumulate where they are moving slowly. This results in emergence of motility induced phase separation (MIPS) where high-density and low-density phases are observed in a large collection of

active particles [? ]. In the following two subsections, we explore MIPS emerging in (a) two dimensional ABP-like particles and (b) particles driven by a Bouali attractor.

#### 1. Two dimensional ABP-like particles

In conventional active matter, ABPs have been shown to undergo MIPS [? ]. By exploring a large collection of two-dimensional ABP-like particles considered in Sec. V A, with added repulsive harmonic interactions as described in Sec. III C, we also obtain MIPS, as shown in Fig. 5 and Supplemental Video S2.

#### 2. Non-equilibrium MIPS

In addition to conventional MIPS, we can also generate more exotic MIPS using a different strange attractor to drive the active particle. For example, by generating an RTP-like particle driven by the Bouali attractor [? ], we obtain the intermittent MIPS behavior shown in Fig. 6 and Supplemental Video S3. As shown in Fig. 4(c) of the main text, the Bouali-attractor driven active particle gives rise to a trajectory where the particle alternates between (i) phases of a long “run”, where the particle spends a long time in ballistic motion at a constant velocity, and (ii) an “explore” phase, where the particle moves around in a localized region. When many such particles with harmonic repulsive interaction (as described in Sec. III C) are initiated at random locations in a square periodic domain with slightly different initial conditions  $((X(0), Y(0), Z(0)) = (-1, 1, 0) + \eta(t)$ , where  $\eta(t)$  is a random number selected uniformly from the interval  $[0, 0.01]$ ), they undergo MIPS where we see regions of high density clusters. The MIPS emerges when the active particles are in the long “run” phase. After some

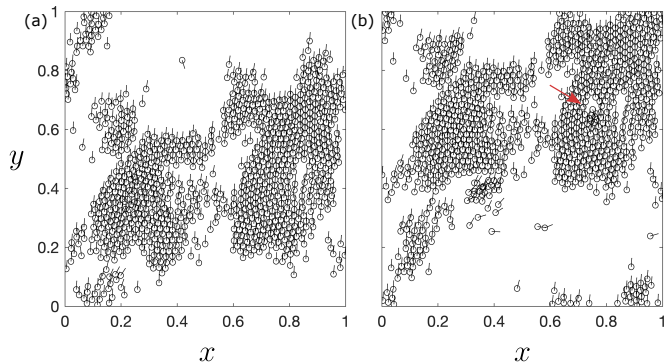


FIG. 7. Two-dimensional flocking with added repulsive harmonic interactions between the active particles (see also Supplemental Video S4). Voids can form in such flocks. This is depicted in (a) and (b), which show the system just before and just after the formation of a void. The parameters of the driving strange attractor are the same as in Fig. 5 of the main text. The other parameters as follows: number of particles is 1000, alignment interaction radius is  $\Delta = 0.05$ , size of each particle is 0.01, weight factor is  $W = 0.9$ , particle velocity is  $u = 1$  and the spring constant for harmonic interactions is  $K = 50$ .

time, when the particles enter the “explore” phase, it results in the disintegration of clusters. This process repeats as particles alternate between the long “run” phase and the “explore” phase, and we obtain oscillations between phases of MIPS-like clustered regions and gas-like phases with no clear large-scale structure.

### C. Two dimensional flocks with repulsive and aligning interactions

In addition to the flocking behavior described in the main text, we can obtain flocking behavior with a crystal-

like arrangement within the flock by including short range repulsive harmonic interactions in addition to the long-range aligning interactions. This is illustrated in Fig. 7 and Supplemental Video S4. These flocks also show a variety of phenomena including voids and defect formation within clusters, merging and disintegration of clusters and soliton-like disturbance propagation of alignments within the cluster.

## SUPPLEMENTAL VIDEOS

**Supplemental Video S1:** Flocking behavior for two-dimensional RTP-like particles driven by the Lorenz attractor with added aligning interactions, as shown in Fig. 5 of the main text.

**Supplemental Video S2:** MIPS for two-dimensional ABP-like particles, as shown in Fig. 5 of this Supplemental Material.

**Supplemental Video S3:** Non-equilibrium MIPS for two-dimensional active particles driven by the Bouali attractor, as shown in Fig. 6 of this Supplemental Material.

**Supplemental Video S4:** Flocking behavior with added short-range repulsive harmonic interactions in addition to the long-range aligning interactions, as shown in Fig. 7 of this Supplemental Material.